DTU Library

Wind tunnel tests of a free yawing downwind wind turbine

Verelst, David Robert; Larsen, Torben J.; van Wingerden, Jan-Willem

Published in:
Journal of Physics: Conference Series (Online)

Link to article, DOI:
10.1088/1742-6596/555/1/012103

Publication date:
2014

Document Version
Publisher's PDF, also known as Version of record

Wind tunnel tests of a free yawing downwind wind turbine

2014 J. Phys.: Conf. Ser. 555 012103

(http://iopscience.iop.org/1742-6596/555/1/012103) doi:10.1088/1742-6596/555/1/012103

Wind tunnel tests of a free yawing downwind wind turbine

[1] **DRS Verelst,** [1] **TJ Larsen and** [2] **JW van Wingerden**

[1] DTU Wind Energy, [2] TU Delft

E-mail: `dave@dtu.dk`

Abstract. This research paper presents preliminary results on a behavioural study of a free yawing downwind wind turbine. A series of wind tunnel tests was performed at the TU Delft Open Jet Facility with a three bladed downwind wind turbine and a rotor radius of 0.8 meters. The setup includes an off the shelf three bladed hub, nacelle and generator on which relatively flexible blades are mounted. The tower support structure has free yawing capabilities provided at the base. A short overview on the technical details of the experiment is given as well as a brief summary of the design process. The discussed test cases show that the turbine is stable while operating in free yawing conditions. Further, the effect of the tower shadow passage on the blade flapwise strain measurement is evaluated. Finally, data from the experiment is compared with preliminary simulations using DTU Wind Energy's aeroelastic simulation program HAWC2.

1. Introduction

The free yawing concept is argued to increase wind turbine robustness by removing the need for an actively controlled yaw system. Reducing the number of failure prone and actively controlled mechanisms should in theory lead to less maintenance actions and reduced downtime. Although not the focus of the current study, a free yawing system might reduce the average operating yaw error due to absence of an error on the wind direction measurement. This could lead to an increase in annual energy yield assuming the average operating yaw error is smaller for a free yawing system. Additionally, a reduced lag between the yaw control action and a wind direction change can be expected for a free yawing system. For this research project, both wind tunnel tests (which were performed in February and April 2012) and simulations are used to evaluate the free yawing concept. The Open Jet Facility of the TU Delft was used for the experiments (see figures 1 and 3 for an overview), and the experiment's design procedure and setup are briefly described here. A preliminary assessment is given on the effect of the tower shadow passage on the blade strain measurement. Finally, the measured free yawing behaviour is compared with simulations using the aeroelastic tool HAWC2 [1].

The free yaw stability of a 3 bladed downwind conceptual wind turbine with a rating of 100 kW has been evaluated using aeroelastic simulations before in [2] and [3].

2. Experimental setup: three bladed, free yawing, downwind turbine

2.1. Overview

Figure 1 presents a general overview of the test setup installed in the OJF wind tunnel. Some key characteristics of the experiment:

Figure 1. General overview of the experimental setup in the OJF at the TU Delft.

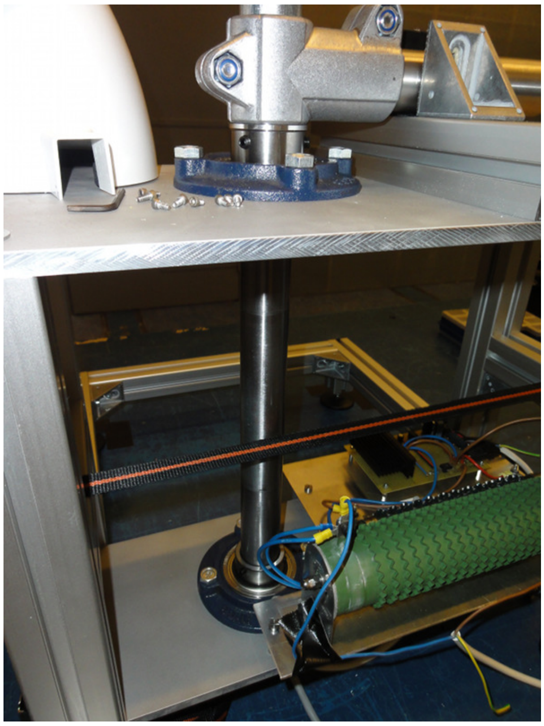

Figure 2. Close up of the free yawing system and electrical generator load.

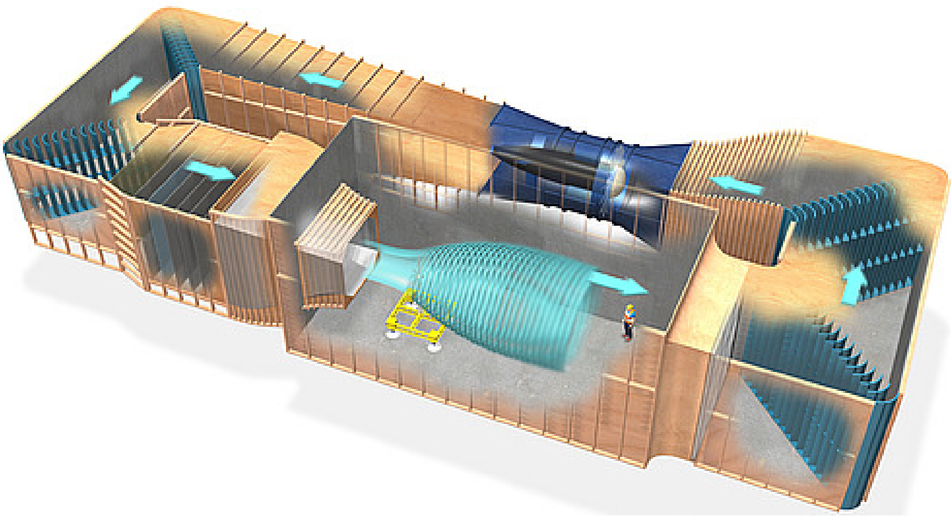

Figure 3. Schematic overview of TU Delft OJF wind tunnel. Key parameters: operational wind speeds from 3 to 25 m/s, and exit nozzle measures 2.8 by 2.8 meters. A much larger test section room facilitates flow expansion around the wind turbine.

- The tower base is suspended on two bearings, allowing the complete tower to yaw (see figure 2). The nacelle is fixed to the tower top.
- In free yawing mode the yaw angle range is approximately -35 to 35 degrees. The yaw angle can be locked or manually controlled in free yaw mode from the control room.

- The generator is connected to a variable electrical load (resistance) for limited torque variability. No active rotor speed control was pursued during the experiments.
- Strain gauges on the tower base in for-aft and side-side directions.
- Strain gauges on two blades (one stiff and one soft blade set) at the root and 30% radius positions. Wireless transmission of data to acquisition pc.
- 3D-accelerometer at the tower top.
- Laser distance meter to measure the yaw angle.
- Wind speed, temperature and static pressure measurements were taken from the available OJF measurement system.

The starting point of the testing hardware is an off the shelf small wind turbine that compromises an aluminium cast nacelle, standard 300 W permanent magnet generator with rectifier, and a hub disc with three mounting points for the blades. The original aluminium extruded blades are replaced by a 55 cm long custom build and relatively flexible blades.

In order to maintain a common optimal tip speed ratios (approximately 6-7), this small wind turbine is designed to operate at optimal conditions at around 450 rpm. Further, a high rotation speed is required to minimize the difference in Reynolds numbers with a full scale turbine. Note that the difference is still significant.

2.2. Blade design

The airfoil selection is based on publicly available airfoil data. The UIUC Low-Speed Airfoil Tests (UIUC LSATs) holds an open repository of numerous wind tunnel test results of 2D airfoil sections [4]. Since the test results will be compared to aeroelastic simulations later on, the airfoil selection is based on the availability of 2D sectional wind tunnel test data at the relevant Reynolds numbers (within the range of 100,000 - 200,000). From the UIUC database [5], the NREL S823 (21% thickness) was selected for the root section, and the NREL S822 (16% thickness) for the tip.

The aerodynamic layout or planform of the blade is designed using HAWTOPT [6]. The optimizer objective is set to maximize power output while varying chord length, airfoil thickness and twist angle (all within given practical boundaries regarding the manufacturing process).

The structural part of the blade is designed with a certain flexibility in mind (translated in a tip deflection constraint) under the given operational conditions. Due to the high rotational speeds and the corresponding centrifugal stiffening this is not a trivial task. Keeping blade mass very low is as crucial as achieving certain stiffness and strength characteristics. The outcome to this problem presents itself as a foam blade with an inner glass-fiber sandwich beam core. The outer foam provides and maintains the aerodynamic shape, and the glass-fiber inner beam delivers strength and stiffness while keeping the mass to an absolute minimum.

3. Tower shadow passage and effect on blade strains

A possible disadvantage of a downwind wind turbine is the effect of tower shadow passage on the blade loading. The current experiment shows that the blade tower shadow passage has a significant effect on the loading, as can be seen in figures 4 and 5. Note that the yaw angle is fixed at 0 degrees. Especially in deep stalled conditions (figure 4) and relatively slow rotation speeds, the effect of tower shadow passage is clearly visible: a sudden drop in the aerodynamical loading triggers a vibration that damps out before the following passage through the tower shadow. Figure 5 shows the same experiment but now at much higher rotational speed and operating at near optimal tip speed ratios.

Due to the high rotational speed the centrifugal forces introduce an additional offset on the blade strain measurements. In theory, the strain gauges on the upper and lower side of the beam should have been mounted with equal distance from the neutral axis. However, the applied production process did not allow such a fine grained control. Additionally, a slight coning angle misalignment introduces a rotating speed dependent flapwise bending moment. Consequently, the strain gauge measurements have a rotor speed dependent component that is independent from the aerodynamics. Further it is noted that due to the significant centrifugal stiffening of the blade the eigenfrequency increases from 12 Hz at low rpm (figure 4) to 62.5 Hz at high rpm (figure 5, although power spectral density analysis of the signal is not shown here).

It is expected that the tower shadow passage will affect mainly the amount of blade fatigue damage. However, the current study does not evaluate any fatigue damage criteria in comparison with an upwind configuration. Future studies should consider a more detailed assessment of the impact of tower shadow passage on the blade fatigue life while comparing upwind and downwind concepts.

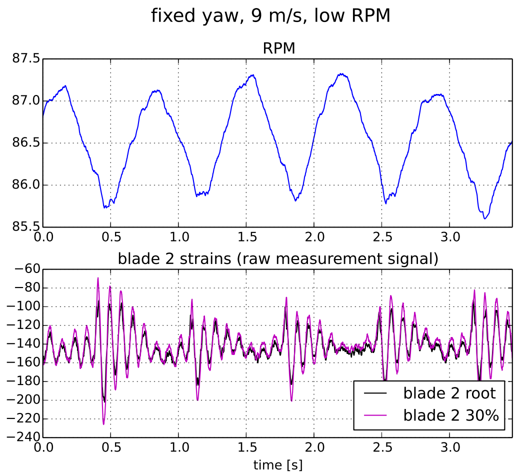

Figure 4. Rotational speed and blade non dimensional strains at deep stall conditions.

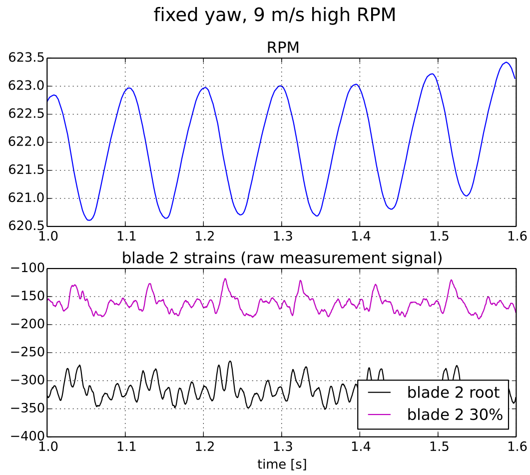

Figure 5. Rotation speed and non dimensional blade strains at near optimal tip speed ratios

4. Free yaw stability in the OJF wind tunnel

Several runs in the wind tunnel are performed to measure yaw stability under varying initial conditions. In figures 6 and 7 the wind turbine is operating in deep stall conditions at low rotational speeds. For figure 7, a positive yaw error of 34 degrees is forced upon the system. After 28 seconds the yaw angle is released, and as a result the corresponding yaw error quickly falls back to 0 degrees. From a stability point of view it can be identified as a favourable overdamped system. However, the 0 degree yaw angle does not correspond to a steady state, and instead it slowly increases. After 60 seconds, there is still no steady state reached. Approaching from the other side, figure 6 shows the response when forcing a negative yaw error on the turbine. After 31 seconds the yaw angle is released, and a steady state yaw error of -23 degrees is reached already at 40 seconds. Note that for both cases the rotor torque is not actively tracked and hence the rotor speed drops due to decreased aerodynamic torque available under yawed inflow conditions. For figure 7 the rotor speed drops to approximately 88 rpm, while in figure 6 it is reduced to 72 rpm.

Although the lack of detailed aerodynamic measurements prevent from drawing any fundamental conclusions, one could make some interesting observations. The yawing moments in deep stall conditions appear to be small for close to zero yaw angles. They are not symmetric and favour a negative steady state yaw angle. The negative steady state yaw error might be caused due to the presence of an unknown horizontal wind shear in the wind tunnel, or the tower shadow passage might introduce a non symmetrical azimuthal dependent blade load distribution before and after tower shadow passage due to dynamical stall effects causing a nonzero yaw moment at a zero yaw inflow angle.

In figure 8, test results are shown for the turbine operating at high rotation speeds close to optimal tip speed ratio. The turbine initial state is in a free steady yawing condition until the yaw angle is forced to -35 degrees just before 10 seconds. At around 20 seconds the turbine is set free to yaw once again and the yaw error quickly falls back to a steady value close 0 degrees. There is no sign of overshoot in the restoring motion. The experiment is repeated in the other direction forcing a yaw angle of +35 degrees (at 35 seconds). A similar response is noted. During yawed operation the aerodynamic torque is reduced significantly resulting in a noticeable drop in rotor speed (approximately 25 %). Although the difference is hardly noticeable, a different steady state yaw angle is reached when coming from the negative or positive forced yaw errors. An initial forced negative yaw error leads to a small negative steady state yaw angle when set free, and this trend is consistent with the deep stall cases (as discussed in the previous paragraph).

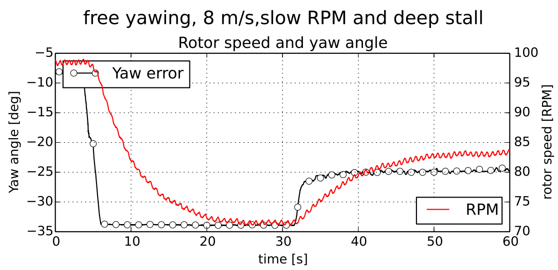

Figure 6. Free yaw stability of a rotor in deep stall conditions, initial yaw error negative.

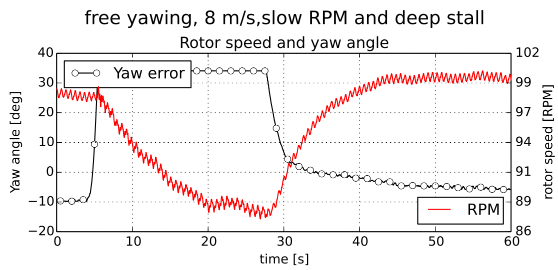

Figure 7. Free yaw stability of a rotor in deep stall conditions, initial yaw error positive.

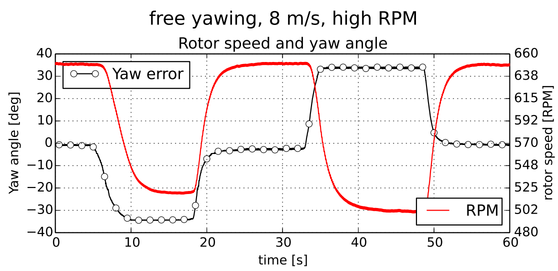

Figure 8. Free yaw stability near optimal tip speed ratios: results from the OJF measurements only.

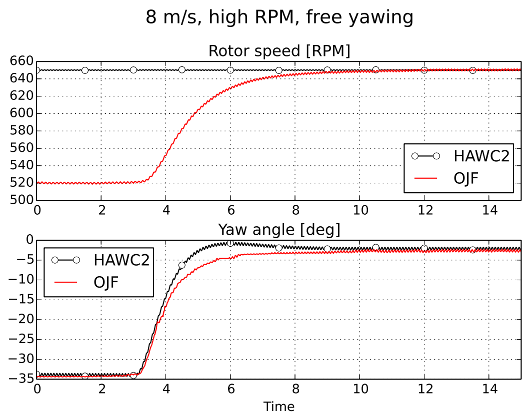

Figure 9. Free yaw stability near optimal tip speed ratios.

5. Modeling the OJF experiment in HAWC2

A very brief overview of HAWC2 is presented here, as well as short description of how a numerical representation of the wind tunnel experiment was created.

HAWC2 uses a multi-body formulation combined with a Timoshenko beam element that allows to account for body flexibility. On the aerodynamical part a classical BEM code is combined with corrections to account for tip losses, tower shadow effects, dynamic inflow and dynamic stall.

For the aerodynamic model, 2D sectional data of the considered airfoils is required. Available wind tunnel data from the UIUC database is extended to cover a broader range of angles of attack using the methods that are described in [7].

The structural model is defined by the cross-sectional beam parameters of each section. For the tubular steel tower these parameters can be obtained relatively easily. However, for the hybrid blade structure (foam combined with glass-fiber sandwich) this problem is less trivial. As a starting point a simplified cross sectional analysis is performed assuming a full foam section with isotropic properties. Next the modulus of elasticity is changed until the simulated blade first flapwise eigenfrequency matches the measured value of the real blades. This matching procedure is used in order to focus this initial investigation on the structural dynamics of the system in HAWC2 rather than including the additional uncertainty and complexity of a more detailed cross sectional analysis.

6. Comparing free yaw behavior: HAWC2 simulations and OJF results

In section 4 the free yaw response of the wind tunnel experiment was discussed. In this section those results are compared with preliminary aeroelastic simulations performed in HAWC2. Note that currently the simulations are limited to constant rotor speed and as a result the rpm variation witnessed in the test results are not replicated in the simulations. However, it does reveal some interesting trends when comparing simulations and experiments.

For the deep stall cases at low rpm (figures 10 and 11) the simulations predict a steady state yaw error close to 0 degrees regardless of the initial forced yaw error and rotor speed. This is not in agreement with the measurements where an asymmetric steady state yaw response was noted. In addition to the short discussion presented on the measurements in section 4, it should be noted that the yawing degree of freedom has zero friction for the simulations. If the yawing moment is very low and close to the friction forces, different steady state angles close to zero might be possible for varying degrees of yaw bearing friction. Future work could consider a yaw bearing friction sensibility analysis in order to assess its effect on steady state free yawing angles for various initial conditions.

At high rotation speeds the experiment only showed a very small negative steady state yaw angle for negative initial yaw angle conditions (figure 8). For the simulations, however, the steady state free yaw angle does not depend on the initial conditions (see 9).

Another observation concerns the dynamic response of the yaw angle. For the three considered cases in figures 9, 10, and 11, simulations show a small overshoot in the yaw angle when going back to zero. This overshoot is not present in the experimental data and suggests there is more damping present in the yawing behaviour. This might be related to the constant simulated rotor speed compared to the rotor speed acceleration when yawing to zero degrees for the experiment.

7. Conclusions and future work

This paper presented preliminary results of a numerical and experimental investigation on the behaviour of a free yawing downwind wind turbine. Although more extensive numerical work remains to clearly explain the free yawing behaviour of the simulations and experiments, following conclusions can be drawn from the presented material:

- A three bladed downwind wind turbine is stable in yaw for the considered test cases.

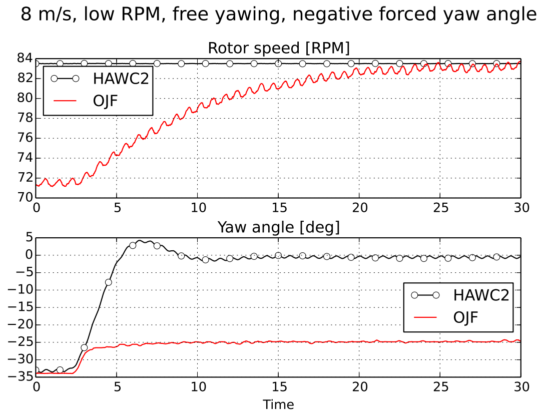

Figure 10. Free yaw stability of a rotor in deep stall conditions, initial yaw error negative.

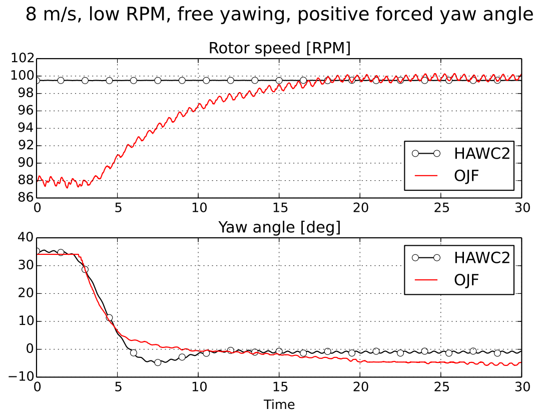

Figure 11. Free yaw stability of a rotor in deep stall conditions, initial yaw error positive.

- When the rotor is in deep stall the free yawing cases are stable, but they operate under a constant yaw error. Simulations do not show the same behaviour: an unaccounted horizontal wind shear in the wind tunnel, or different dynamic stall and tower shadow interactions in the numerical model could potentially cause this difference.
- As expected, tower shadow passage has a significant effect on blade loading. A fatigue load comparison between an upwind and downwind rotor is suggested to quantify its effect.
- This paper does not study how free yawing affects the dynamical behaviour of the induction at the rotor plane. Dynamic inflow, yaw corrections, and a rapidly changing wake are believed to interact, but those interactions are not accounted for in the presented simulations, and they should be studied in greater detail in the future.

Acknowledgments
This research is partly funded by EU 7th Framework Marie Curie IAPP grant #230698 "WINDFLOWER" and the NWO Veni Grant #11930 "Reconfigurable Floating Wind Farms".

References
[1] Larsen T J 2009 HAWC2 user manual Tech. Rep. Risø-R-1597(ver. 3-9)(EN) Risø National Laboratory Denmark URL `http://130.226.56.153/rispubl/reports/ris-r-1597.pdf`

[2] Verelst D R and Larsen T J 2010 Yaw stability of a free-yawing 3-bladed downwind wind turbine *EAWE 6th PhD Seminar* (Trondheim) URL `http://orbit.dtu.dk/en/publications/id(58599368-8825-45f0-bb18-d48b863008b5).html`

[3] Picot N, Verelst D R and Larsen T J 2011 Free yawing stall-controlled downwind wind turbine with swept blades and coned rotor *EWEA Annual Event 2011 Brussels* (EWEA)

[4] Selig 2012 UIUC low-speed airfoil tests URL `http://www.ae.illinois.edu/m-selig/pd.html`

[5] Selig M, Lyon C, Giguere P, Ninham C and Guglielmo J 1995 *Summary of low-speed airfoil data* vol 1 (SoarTech Publications) ISBN ISBN 0964674718 URL `http://www.ae.illinois.edu/m-selig/uiuc_lsat/Low-Speed-Airfoil-Data-V1.pdf`

[6] Fuglsang P, Bak C, Schepers J G, Bulder B, Cockerill T T, Claiden P, Olesen A and van Rossen R 2002 *Wind Energy* **5** 261–279 ISSN 1099-1824 URL `http://onlinelibrary.wiley.com/doi/10.1002/we.61/abstract`

[7] Montgomerie B 2004 Methods for root effects, tip effects and extending the angle of attack range to +-180 deg, with application to aerodynamics for blades on wind turbines and propellers Tech. Rep. FOI-R–1305–SE FOI - Swedish Defence Research Agency URL `http://www2.foi.se/rapp/foir1305.pdf`